Analysis of Mode Characteristics for Deformed Square Resonators by FDTD Technique

Qin Chen, Yong-Zhen Huang, *Senior Member, IEEE*, and Li-Juan Yu

***Abstract*—The mode frequencies and quality factors (Q-factors) in two-dimensional (2-D) deformed square resonators are analyzed by finite-difference time-domain (FDTD) technique. The results show that the deformed square cavities with circular and cut corners have larger Q-factors than the perfect ones at certain conditions. For a square cavity with side length of 2 μm and refractive index of 3.2, the mode Q-factor can increase 13 times as the perfect corners are replaced by a quarter of circle with radius of 0.3 μm. Furthermore the blue shift with the increasing deformations is found as a result of the reduction in effective resonator area. In square cavities with periodic roughness at sidewalls which maintains the symmetry of the square, the Q-factors of the whisperin gallery (WG)-like modes are still one order of magnitude larger that those of non-WG-like modes. However, the Q-factors of these two types of modes are of the same order in the square cavity with random roughness. We also find that the rectangular and rhombic deformation largely reduce the Q -factors with the increasing offset and cause the splitting of the doubly degenerate modes due to the breaking of certain symmetry properties.**

***Index Terms*—Finite-difference time-domain (FDTD) methods, optical resonators, modeling.**

I. Introduction

RECENTLY, square optical microcavities have attracted great attention due to their potential application for microlasers and high finesse add–drop filters [1]–[12]. Manolatou first discussed the whispering gallery (WG)-like modes in a square cavity and the operation principle of resonant channel add–drop filters based on these modes. Poon *et al.* observed the multimode resonance in the elastic scattering of 200-μm square-shaped μ-cavities in fused silica and simulated the mode coupling in planar waveguide-coupled perfect and corner-cut square microcavities [2], [4], [5]. Lohmeyer used the mode expansion method to investigate the rectangular microresonators add–drop filters and concluded that the cavity should be slightly elongated along the waveguides to compensate for the loss raised by the breaking of C_4 symmetry due to the presence of bus waveguide [3]. Moon *et al.* achieved the WG mode lasing in a gain-coated square microcavity with round corners and observed single spatial mode selection in a layered square microcavity laser [6], [7]. Boriskina *et al.* analyzed the mode characteristics in square cavities with imperfect boundary, which maintains the symmetry properties of the square cavity [8], [9]. Some theoretical analysis based on group theory and numerical simulation by finite-difference time-domain (FDTD) of the mode characteristics for microsquare resonators were proposed by Huang *et al.* [10]–[13], which concluded that the WG-like modes in perfect microsquare cavity have high Q-factor and twice free spectral range (FSR) as that of the microdisk with the same size. However, the fabrication of a perfect square-shape cavity in micrometer scale is very difficult. We do not know whether the double FSR still exists in the deformed square cavity or not. So the modes characteristic in the deformed square cavities is required to be investigated in detail. In this paper, the variations of mode frequencies and mode Q-factors in square cavities with the imperfection include circular and cut corners, periodic and random roughness at sidewalls, rhombic and rectangular deformation are discussed. The results show that the deformed square cavities with circular and cut corners have one order of magnitude larger Q-factors than those of the perfect ones at certain conditions. Furthermore, the blue shift with the increasing deformation is observed as a result of the reduction in effective resonator area. In square cavities with periodic roughness at sidewalls, the Q-factors exponentially decrease with the increasing perturbation amplitude and the variations of the mode wavelengths are linear. Furthermore, the Q-factors of the WG-like modes are still one order of magnitude larger that those of non-WG-like modes. In the square cavity with random roughness, which breaks the symmetry properties of the perfect square cavity, the Q-factors of these two types of modes are of the same order. We also find that the rhombic and rectangular deformations reduce the Q-factors largely with the increasing offset and cause the splitting of the doubly degenerate modes.

The outline of the paper is as follows. In Section II, we analyze the deformed cavity with circular and cut corners and show the variations of mode Q-factors and frequencies with the offset of the deformation. In Section III, we simulate the square cavity with harmonic and random fluctuation at the sidewalls and show the effect of perturbation amplitude to the modes characteristics. In Section IV we investigate two deformations include rhombus and rectangle, which break certain symmetry properties of the perfect square cavities. The conclusion is given in the Section V.

II. Deformed Square Cavity With Circular and Cut Corners

We choose a two-dimensional (2-D) square cavity with $a = 2\,\mu$m and $n = 3.2$ as the perfect cavity, where a is the side length and n is the effective refractive index of the square cavity [9]. Then we add various deformations to the perfect cavity. Only

Manuscript received July 25, 2005; revised September 28, 2005. This work was supported in part by the National Nature Science Foundation of China under Grant 60225011 and the project of "863" plan under Grant 2003AA311070.

The authors are with the State Key Laboratory on Integrated Optoelectronics, Institute of Semiconductors, Chinese Academy of Sciences, Beijing 100083, China (e-mail: chenqin@red.semi.ac.cn; yzhuang@red.semi.ac.cn; ylj@red.semi.ac.cn).

Digital Object Identifier 10.1109/JQE.2005.859912

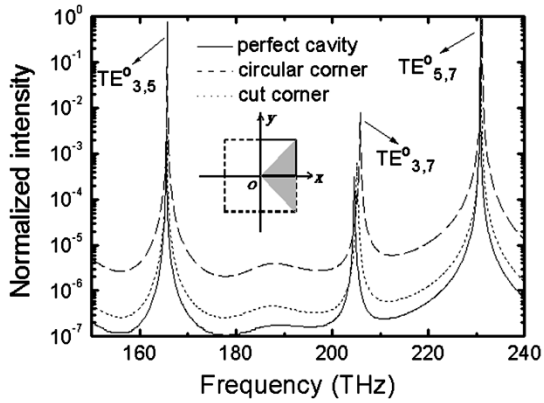

Fig. 1. Intensity spectra obtained by 2-D FDTD simulation and the Padé approximation under both symmetric conditions relative to the x and y axes. The solid line, dashed line, and dotted line are according to perfect square cavity, circular corner cavity ($R = 0.3\ \mu$m) and cut corner cavity (cut length $= 0.19\ \mu$m), respectively. The mode numbers is also indicated at each peak in the spectra. The schematic diagram of a 2-D square cavity is shown in the inset, which is plotted by the dashed lines. A quarter of square is plotted by solid line is chosen as the calculating window in FDTD.

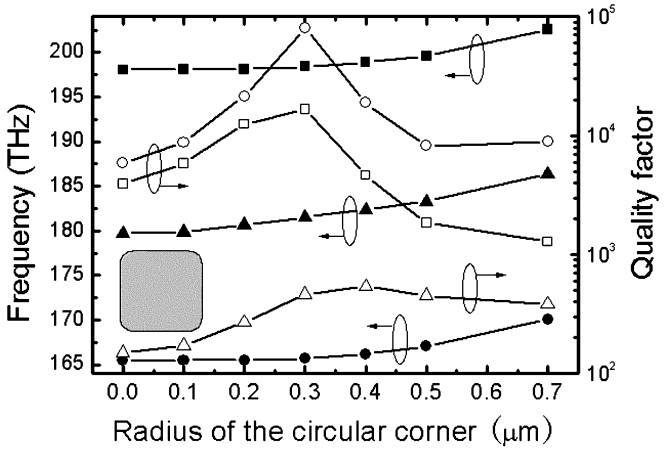

Fig. 2. Mode frequencies and Q-factors versus the radius in circular corner square cavity, where the circles, squares and triangles are according to $\mathrm{TE}^{\circ}_{(3,5)}$, $\mathrm{TE}^{\circ}_{(4,6)}$, and $\mathrm{TE}_{4,5}$, and solid and open shapes are for mode frequencies and Q-factors, respectively. The schematic diagram of circular corner square cavity with $R = 0.3\ \mu$m is shown in the inset.

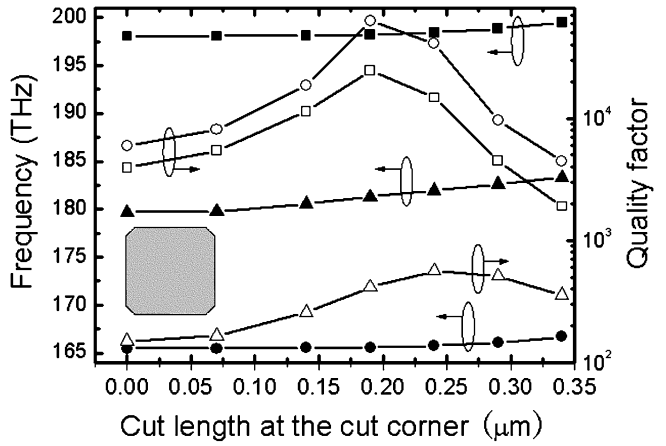

Fig. 3. Mode frequencies and Q-factors versus the cut-length at sides in cut corner square cavity. The sign is the same as Fig. 2. The schematic diagram of cut corner square cavity with cut length $0.19\ \mu$m is shown in the inset.

the TE modes are analyzed here. The details in the numerical simulation can be obtained from [13].

In this section, we calculate the mode frequencies and Q-factors of the WG-like modes $\mathrm{TE}^{\circ}_{(3,5)}$ and $\mathrm{TE}^{\circ}_{(4,6)}$ in the deformed square cavity with circular and cut corners, respectively, where "o" represents odd states relative to the diagonal mirror planes of the square cavity. The accidentally degenerate modes of the WG-like modes are not considered, whose field distributions are symmetric and have one order of magnitude smaller Q-factors [11]. The non-WG like mode $\mathrm{TE}_{4,5}$ is also calculated for comparison, whose mode frequency is located in the midst of the frequencies of $\mathrm{TE}^{\circ}_{(3,5)}$ and $\mathrm{TE}^{\circ}_{(4,6)}$, but one order of magnitude smaller Q-factors. The radius of circular corners R is set to be 0.1–0.7 μm and the cut length of the side at corners is 0.1–0.3 μm, respectively. The space step in FDTD simulating is set to be 0.01 μm.

The schematic diagram of a 2-D square cavity is shown in the inset of Fig. 1, which is plotted by the dashed lines. A quarter of the square resonator drawn by solid lines is used for 2-D FDTD simulation under different symmetric conditions [13]. In Fig. 1 we plot the intensity spectra of the perfect square cavity (solid line), circular corner (dash line) and cut corner cavity (dot line), which is calculated under both antisymmetry boundary to magnetic field component H_z in the 2-D FDTD simulation. The mode numbers (p, q) of each peak are identified by comparing with 2-D analytical results [11]. We can see that the two deformations cause frequencies shift and the variations of the Q-factors.

In Fig. 2, we show the frequencies and Q-factors versus the radius in circular corner square cavity, where the circles, squares and triangles are according to $\mathrm{TE}^{\circ}_{(3,5)}$, $\mathrm{TE}^{\circ}_{(4,6)}$, and $\mathrm{TE}_{4,5}$, and solid and open shapes are for mode frequencies and Q-factors, respectively. From the variation of Q-factors with the radius, we find the deformation even increases the Q-factors at certain region of radius. The largest Q-factors of $\mathrm{TE}^{\circ}_{(3,5)}$ and $\mathrm{TE}^{\circ}_{(4,6)}$ at $R = 0.3\ \mu$m are over 13 times and four times as larger as those of the perfect square cavity, respectively. The Q-factor of $\mathrm{TE}_{4,5}$ at $R = 0.4\ \mu$m increase four times, which is also one order of magnitude smaller than those of the WG-like mode. We also can see the blue shift of the three modes with the increasing radius of circular corners. This relation can be explained as that the effective resonator area of circular corner square cavity with larger radius is smaller, which results in the reduction of mode wavelengths. At $R = 0.7\ \mu$m, the mode frequencies shift is 3 THz for $\mathrm{TE}^{\circ}_{(3,5)}$ and 4 THz for $\mathrm{TE}^{\circ}_{(4,6)}$, respectively. For the case of cut corner square cavity shown in Fig. 3, we also observe the similar variation of mode frequencies and Q-factors. The largest Q-factors of $\mathrm{TE}^{\circ}_{(3,5)}$ and $\mathrm{TE}^{\circ}_{(4,6)}$ with 0.19-μm cut length at side are over ten times and six times as larger as those of the perfect square cavity, respectively.

We think the enhanced confinement of the resonant modes in circular and cut corner square cavities at certain conditions is the result of the compressed radiation at the corners due to the deformation. We show the normalized field pattern of the magnetic field component H_z for $\mathrm{TE}^{\circ}_{(3,5)}$ modes in Fig. 4, which is obtained by 2-D FDTD simulation. Fig. 4(a)–(c) is according to the perfect square, circular corner cavity ($R = 0.3\ \mu$m) and

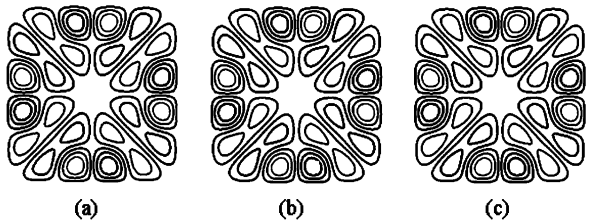

Fig. 4. Field pattern of the magnetic field component H_z for $\mathrm{TE}^{\circ}_{(3,5)}$ modes in (a) perfect square, (b) circular corner cavity, and (c) cut corner cavity obtained by 2-D FDTD simulation.

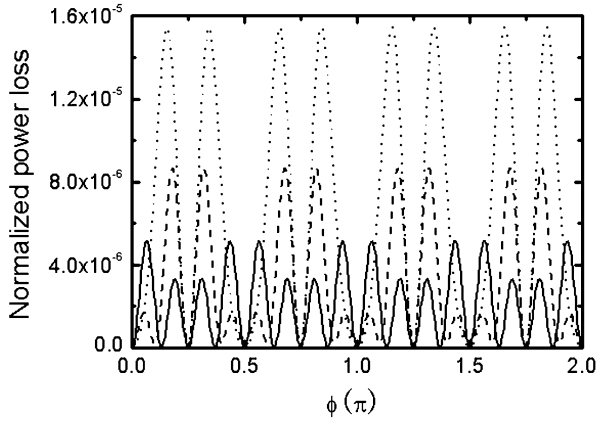

Fig. 5. Power angular spectra of the $\mathrm{TE}^{\circ}_{(3,5)}$ modes in the perfect square cavity (dot line, the intensity was reduced by five times), circular corner cavity (solid line) and cut corner cavity (dashed line).

cut corner cavity (cut length$= 0.19\ \mu$m), respectively. We can see the deformation of cavity do not modify the field pattern largely. Only very small difference at the corner is observed. In Fig. 5, we show the power angular spectra of the $\mathrm{TE}^{\circ}_{(3,5)}$ in the three structures based on far field emission [10]. Dotted line, solid line and dashed line are according to the perfect square, circular corner cavity ($R = 0.3\ \mu$m) and cut corner cavity (cut length $= 0.19\ \mu$m), respectively. The intensity of the perfect square shown in the figure is reduced by five times. We can see the escape power in the three structures are all zero at the angles of $\Phi = \pi/4, 3\pi/4, 5\pi/4$, and $7\pi/4$, i.e., in the direction of the square diagonals. It is because that the field distributions of WG-like modes are antisymmetric according to the diagonals. The power escaped from perfect cavity is the largest and that from circular corner cavity is the smallest. We conclude that the two deformations do not break the characteristics of the WG-like modes and even reduce the radiation intensity at certain conditions. In the micrometer scale fabrication of semiconductor microcavity, the sharp angle at the corners of square cavity is difficult to maintain in the process such as photolithography and etching. Now the enhanced confinement of the deformed square cavity with optimized parameters can release the fabrication difficulty to achieve high Q-factors resonant modes lasing and not degrade the double FSR formed by the high-Q WG-like modes.

III. Deformed Square Cavity With Roughness at the Sidewalls

In this section, we investigate the mode characteristics in a square cavity with periodic and random fluctuation at the sidewalls with different perturbation amplitudes. In the FDTD simulation, the fluctuated boundary of the square cavity is described as $P(x) = y_0 + F(x)$, where y_0 is the smooth sidewall position, x is the position in the sidewall, and $F(x)$ is the fluctuation. For the cosinoidal fluctuation, we assume the fluctuation to be $F(x) = \delta\cos(2\pi vx/a)$, where δ is the perturbation amplitude, a is the side length of square cavity and v is the period number (The larger v means the faster variation at the sidewalls). For the random fluctuation, we assume $F(x)$ to be of the form of Gaussian statistics with a zero mean value and a correlation, $\langle F(x)F(x')\rangle = \sigma^2\exp[-(x-x')^2/l^2]$, where σ is the root-mean-square (rms) height and l is the correlation length along the x-direction. The Monte Carlo method is used to construct $F(x)$ [14]. We can see the symmetry properties of the perfect square cavity are maintained in the periodic deformed cavity, so a quarter cavities are used in the FDTD simulation as that in Section II. However, the symmetry properites are broken in the deformed cavity with random roughness at the sidewalls, the whole cavity is used in simulation.

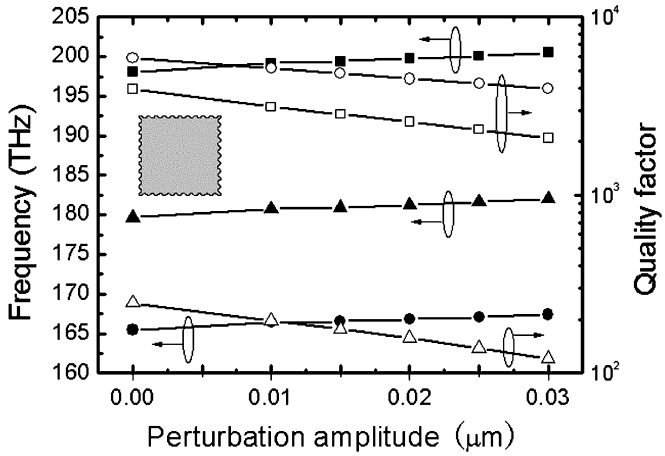

Fig. 6. Mode frequencies and Q-factors versus the perturbation amplitude in deformed square cavity with period roughness at sidewalls and period number $v = 10$. The sign is the same as Fig. 2. The inset is a square cavity with period roughness ($\delta = 0.03\ \mu$m and $v = 10$) at sidewalls.

In Fig. 6, we show the mode frequencies and Q-factors of $\mathrm{TE}^{\circ}_{(3,5)}, \mathrm{TE}^{\circ}_{(4,6)}$, and $\mathrm{TE}_{4,5}$ versus the perturbation amplitude δ, where $v = 10$. We can see the exponentially decreasing of the Q-factors and the linearly increasing of mode frequencies with the increasing perturbation amplitude, which is in agreement with the results in [8]. The larger perturbation causes the stronger scattering, which reduced the Q-factors exponentially with the increasing perturbation amplitude. So a key issue to achieve a high quality microsquare resonator is to compress the roughness at the sidewalls, which forms in the photolithography and etching process. Except the roughness region, the effective resonator area of square cavity with larger perturbation amplitude is smaller, which results in the blue shift like the circular corner and cut corner cases. We observe that the Q-factor of the non-WG-like mode $\mathrm{TE}_{4,5}$ is one order of magnitude smaller than those of WG-like modes and the twice FSR as that determined by cavity length is maintained.

In Fig. 7, we show the mode frequencies and Q-factors of $\mathrm{TE}_{3,5}, \mathrm{TE}_{4,6}$, and $\mathrm{TE}_{4,5}$ versus the rms height σ, where $l = 0.1\ \mu$m. We can see that the obvious difference in Fig. 7 from the Fig. 6, where the Q-factors of original high-Q WG-like modes

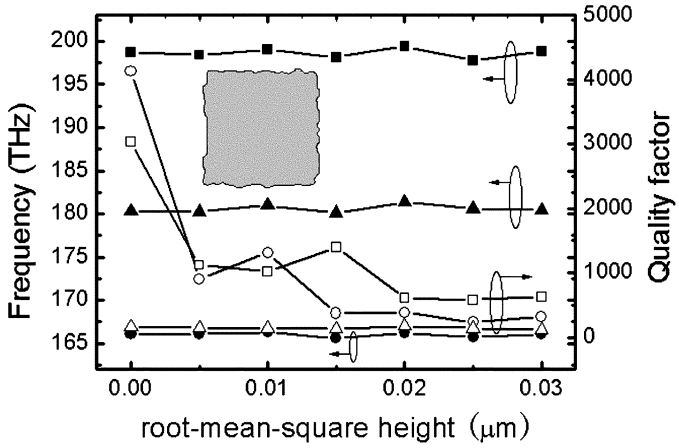

Fig. 7. Mode frequencies and Q-factors versus the rms height in deformed square cavity with random roughness at sidewalls, where the correlation length $l = 0.1$ μm. The sign is the same as Fig. 2. The schematic diagram of a square cavity with $\sigma = 0.02$ μm and $l = 0.1$ μm is shown in the inset.

$\mathrm{TE}_{3,5}$ and $\mathrm{TE}_{4,6}$ decrease to the values of the same order of that of $\mathrm{TE}_{4,5}$. We consider that it is because the random roughness breaks the symmetry along the diagonals, which is the base of the high-Q WG-like modes in the perfect square cavity.

IV. Deformed Square Cavity With Rhombus and Rectangle Shape

In the above discussions, all the deformations maintain the symmetry properties of the perfect square cavity except the deformed square cavity with random roughness at the sidewalls. In this section, we investigate two other deformations of rhombic and rectangular shape, which break the symmetry at the perpendicular bisector of the sides and symmetry along the diagonals, respectively. Furthermore, the C_4 symmetry is broken in both cases. The two deformations are easily happened in wet etching because of the anisotropy of the acid solution.

For the rhombic cavity, the symmetry properties along the perpendicular bisector of the sides are broken. So we can not use a quarter cavities shown by solid line in the inset of Fig. 1 as the calculating window. We use another quarter cavities formed by one side and two diagonals as the calculating window, which is shown by the shadow region in the inset of Fig. 1. We exploit antisymmetric properties to the magnetic field vectors at the diagonals to excite only the odd states (WG-like modes). In Fig. 8, we show the mode frequencies and Q-factors of the WG-like modes $\mathrm{TE}^{\circ}_{(3,5)}$ and $\mathrm{TE}^{\circ}_{(4,6)}$ versus the acute angle in rhombic cavity, where the abscissa represents the value of the acute angle of rhombus. We can see the Q-factors drop down quickly with the increasing rhombic deformation. It can be understood as that the reflective angle at one side of the rhombus may be less than the totally reflective angle after several reflections, not as the case of the square cavity, where the reflective angle is maintained at 45°. So the confinement of electromagnetic wave is not as well as that in square cavity.

In the rectangular cavity, the symmetry properties to the perpendicular bisector of the sides are maintained, we simulate the structure by using a quarter cavities as that described in Section II. However, the symmetry properties to the diagonals

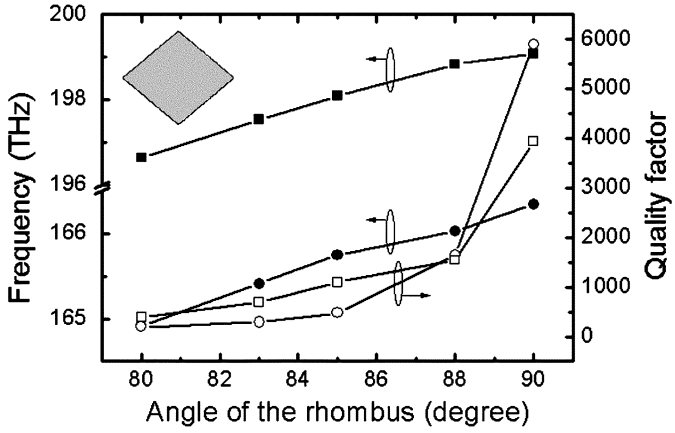

Fig. 8. Mode frequencies and Q-factors of $\mathrm{TE}^{\circ}_{(3,5)}$ and $\mathrm{TE}^{\circ}_{(4,6)}$ versus the acute angle in a rhombus. The sign is the same as Fig. 2. The schematic diagram of rhombic cavity with $\theta = 80^{\circ}$ is shown in the inset.

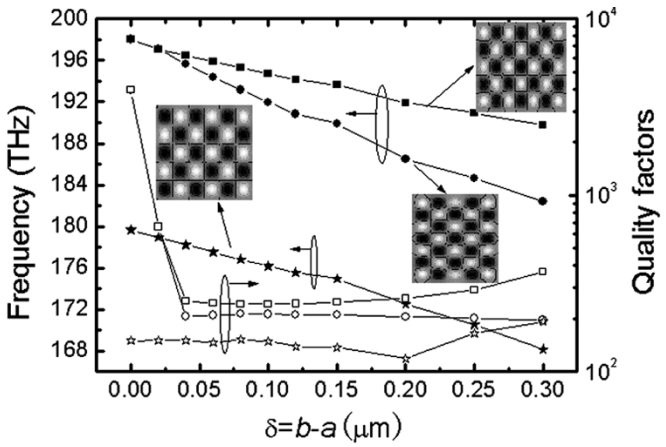

Fig. 9. Mode frequencies and Q-factors versus the difference δ of side lengths in a rectangle, where the squares, circles and stars are according to $\mathrm{TE}_{4,6}$, $\mathrm{TE}_{6,4}$, and $\mathrm{TE}_{4,5}$, and solid and open shape is for mode frequencies and Q-factors, respectively. The field distribution of H_z of the three modes in rectangle cavity with $\delta = 0.1$ μm is shown in the inset, respectively.

are broken. The WG-like modes with antisymmetric magnetic field distribution and their accidentally degenerate modes do not exist. Only the modes like $\mathrm{TE}_{4,6}$ and $\mathrm{TE}_{6,4}$ are supported in this structure. In Fig. 9, we show the mode frequencies and Q-factors of $\mathrm{TE}_{4,6}$, $\mathrm{TE}_{6,4}$, and $\mathrm{TE}_{4,5}$ versus the difference δ of side lengths in a rectangle. The field distributions of H_z of the three modes in a rectangle cavity with $\delta = 0.1$ μm are shown in the inset. We can see $\mathrm{TE}_{4,6}$ and $\mathrm{TE}_{6,4}$ are degenerate in perfect square cavity and split with the increasing difference of the side lengths (The odd states of the combination of $\mathrm{TE}_{4,6}$ and $\mathrm{TE}_{6,4}$ modes in perfect square cavity are just the WG-like mode $\mathrm{TE}^{\circ}_{(4,6)}$ [11]). Furthermore the Q-factors drop from 4000 to 200 when δ increases from zero to 0.04 μm. It is because that the deformation breaks the symmetry properties to the diagonals, which are the base of the high-Q WG-like modes with antisymmetric field distribution according to diagonals in square cavity. When δ is larger than 0.04 μm, the Q-factors tend to stability around 200. For $\mathrm{TE}_{4,5}$, the variation of the Q-factors is much smaller. The value is basically around 150. So we can see the modes with even sum of mode numbers (WG-like modes belong to) in the rectangular cavity have Q-factors with the same order

of magnitude as those modes with odd sum. We think the deformations such as rectangular deformation and random roughness discussed above are the reason that the mode intervals in the experiment results of Poon agree with the ray optics theory which is decided by cavity length [2].

V. Conclusion

We analyzed the mode characteristics in 2-D deformed square resonators by FDTD technique. We find the anomalous increase of the mode Q-factor in circular corner and cut corner square cavity. The results show that the Q-factor of $\mathrm{TE}_{3,5}^{\circ}$ mode in circular corner square cavities ($R = 0.3\ \mu$m) with side length $a = 2\ \mu$m and refractive index $n = 3.2$ increases 13 times as that of the perfect cavity. In the case of cut corner square cavity, the largest enhancement attains ten times with cut length $= 0.19\ \mu$m. Furthermore the blue shift with the increasing deformations is observed as a result of the reduction in the effective resonator area. In square cavities with periodic roughness at sidewalls, the Q-factors of the WG-like modes are still one order of magnitude larger that those of non-WG-like modes. However, the Q-factors of these two types of modes are of the same order in the square cavity with random roughness. At last the rectangular and rhombic deformations are found to be the severe problems in the fabrication of square cavity, which largely reduce the Q-factors with the increasing offset. Furthermore the rectangular deformation splits the degenerate modes and reduces the mode interval to a half of that in perfect square cavity, which is decided by high-Q WG-like modes. We conclude that the twice FSR as that determined by cavity length maintains only in the deformed cavity that maintains the symmetry properties to the diagonals of the perfect square.

References

[1] C. Manolatou, M. J. Khan, S. Fan, P. R. Villeneuve, H. A. Haus, and J. D. Joannopoulos, "Coupling of modes analysis of resonant channel add–drop filters," *IEEE J. Quantum Electron.*, vol. 35, no. 9, pp. 1322–1331, Sep. 1999.

[2] A. W. Poon, F. Courvoisier, and R. K. Chang, "Multimode resonances in square-shaped optical microcavities," *Opt. Lett.*, vol. 26, pp. 632–634, 2001.

[3] M. Lohmeyer, "Mode expansion modeling of rectangular integrated optical microresonators," *Opt. Quantum Electron.*, vol. 34, pp. 541–557, 2002.

[4] C. Y. Fong and A. W. Poon, "Mode field patterns and preferential mode coupling in planar waveguide-coupled square microcavities," *Opt. Exp.*, vol. 11, pp. 2897–2904, 2003.

[5] ——, "Planar corner-cut square microcavities: Ray optics and FDTD analysis," *Opt. Exp.*, vol. 12, pp. 4864–4874, 2004.

[6] H. J. Moon, K. An, and J. H. Lee, "Single spatial mode selection in a layered square microcavity laser," *Appl. Phys. Lett.*, vol. 82, p. 2963, 2003.

[7] H. J. Moon, S. P. Sun, G. W. Park, J. H. Lee, and K. An, "Whispering gallery mode lasing in a gain-coated square microcavity with round corners," *Jpn. J. Appl. Phys.*, vol. 42, pp. L652–654, 2003.

[8] S. V. Boriskina, T. M. Benson, P. Sewell, and A. I. Nosich, "Spectral shift and Q change of circular and square-shaped optical microcavity modes due to periodic sidewall surface roughness," *J. Opt. Soc. Amer. B*, vol. 21, pp. 1792–1796, 2004.

[9] ——, "Optical modes in 2-D imperfect square and triangular microcavities," *IEEE J. Quantum Electron.*, vol. 41, no. 6, pp. 857–862, Jun. 2005.

[10] W. H. Guo, Y. Z. Huang, Q. Y. Lu, and L. J. Yu, "Whispering-gallery-like modes in square resonators," *IEEE J. Quantum Electron.*, vol. 39, no. 9, pp. 1106–1110, Sep. 2003.

[11] ——, "Modes in square resonators," *IEEE J. Quantum Electron.*, vol. 39, no. 12, pp. 1563–1566, Dec. 2003.

[12] ——, "Mode quality factor based on far-field emission for square resonators," *IEEE Photon. Technol. Lett.*, vol. 16, no. 2, pp. 479–481, Feb. 2004.

[13] Q. Chen, Y. Z. Huang, W. H. Guo, and L. J. Yu, "Analysis of modes in a freestanding microsquare resonator by 3-D finite-difference time-domain simulation," *IEEE J. Quantum Electron.*, vol. 41, no. 7, pp. 997–1001, Jul. 2005.

[14] B. J. Li and P. L. Liu, "Numerical analysis of microdisk lasers with rough boundaries," *IEEE J. Quantum Electron.*, vol. 33, no. 5, pp. 791–795, May 1997.

Qin Chen was born in Hubei Province, China, in 1979. He received the B.Sc. degree in physics from Wuhan University, Wuhan, China, in 2001. He is currently working toward the Ph.D. degree at the Institute of Semiconductors, Chinese Academy of Sciences, Beijing, China, and studying the FDTD simulation and fabrication of microcavities and photonic crystals.

Yong-Zhen Huang (M'95–SM'01) was born in Fujian Province, China, in 1963. He received the B.Sc., M.Sc., and Ph.D. degrees in physics from Peking University, Beijing, China, in 1983, 1986, and 1989, respectively.

In 1989, he joined the Institute of Semiconductors, Chinese Academy of Sciences, Beijing, China, where he worked on the tunneling time for quantum barriers, asymmetric Fabry–Pérot cavity light modulators, and VCSELs. In 1994, he was a Visiting Scholar at BT Laboratories, Ipswich, U.K., where he was involved in the fabrication of the 1550-nm InGaAsP VCSEL. Since 1997, he has been a Professor with the Institute of Semiconductors, Chinese Academy of Sciences, and is the Director of the Optoelectronic Research and Development Center. His current research interests involved microcavity lasers, semiconductor optical amplifiers, and photonic crystals.

Li-Juan Yu was born in Heilongjiang Province, China, in 1963. She received the B.S. and M.Sc. degrees in solid physics from Jilin University, Changchun, China, in 1986 and 1989, respectively, and the Ph.D. degree in microelectronics from Xi'an Jiaotong University, Xi'an, China, in 2000.

She joined the Institute of Semiconductors, Chinese Academy of Sciences, Beijing, China, in 2000, working on the material growth by MOCVD and the fabrication process of semiconductor optical amplifier. She is currently an Associate Research Professor at the Institute of Semiconductors, Chinese Academy of Sciences, with the research interest in the material growth and the process techniques for optoelectronic devices.